













## RESEARCH ARTICLE

# Dendritic spine loss in epileptogenic Type II focal cortical dysplasia: Role of enhanced classical complement pathway activation

Laura Rossini<sup>1</sup>  | Dalia De Santis<sup>1</sup>  | Erica Cecchini<sup>1</sup> | Cinzia Cagnoli<sup>1</sup>  |  
 Emanuela Maderna<sup>2</sup>  | Daniele Cartelli<sup>3</sup>  | Bryan Paul Morgan<sup>4</sup>  |  
 Megan Torvell<sup>4</sup>  | Roberto Spreafico<sup>1</sup>  | Roberta di Giacomo<sup>1</sup>  | Laura Tassi<sup>5</sup>  |  
 Marco de Curtis<sup>1</sup>  | Rita Garbelli<sup>1</sup> 

<sup>1</sup>Epilepsy Unit, Fondazione IRCCS Istituto Neurologico Carlo Besta, Milan, Italy

<sup>2</sup>Division of Neurology V and Neuropathology, Fondazione IRCCS, Istituto Neurologico Carlo Besta, Milan, Italy

<sup>3</sup>Neuroalgology Unit, Fondazione IRCCS Istituto Neurologico "Carlo Besta", Milan, Italy

<sup>4</sup>UK Dementia Research Institute, Cardiff University, Cardiff, UK

<sup>5</sup>"Claudio Munari" Epilepsy Surgery Center, GOM Niguarda Hospital, Milan, Italy

## Correspondence

Laura Rossini, Epilepsy Unit, Fondazione IRCCS Istituto Neurologico C. Besta, Via Amadeo, 42, 20133 Milano, Italy.  
 Email: [laura.rossini@istituto-besta.it](mailto:laura.rossini@istituto-besta.it)

## Funding information

AICE-FIRE; Italian Ministry of Health, Grant/Award Number: RF-2016-02362195

## Abstract

Dendritic spines are the postsynaptic sites for most excitatory glutamatergic synapses. We previously demonstrated a severe spine loss and synaptic reorganization in human neocortices presenting Type II focal cortical dysplasia (FCD), a developmental malformation and frequent cause of drug-resistant focal epilepsy. We extend the findings, investigating the potential role of complement components C1q and C3 in synaptic pruning imbalance. Data from Type II FCD were compared with those obtained in focal epilepsies with different etiologies. Neocortical tissues were collected from 20 subjects, mainly adults with a mean age at surgery of 31 years, admitted to epilepsy surgery with a neuropathological diagnosis of: cryptogenic, temporal lobe epilepsy with hippocampal sclerosis, and Type IIa/b FCD. Dendritic spine density quantitation, evaluated in a previous paper using Golgi impregnation, was available in a subgroup. Immunohistochemistry, in situ hybridization, electron microscopy, and organotypic cultures were utilized to study complement/microglial activation patterns. FCD Type II samples presenting dendritic spine loss were characterized by an activation of the classical complement pathway and microglial reactivity. In the same samples, a close relationship between microglial cells and dendritic segments/synapses was found. These features were consistently observed in Type IIb FCD and in 1 of 3 Type IIa cases. In other patient groups and in perilesional areas outside the dysplasia, not presenting spine loss, these features were not observed. In vitro treatment with complement proteins of organotypic slices of cortical tissue with no sign of FCD induced a reduction in dendritic spine density. These data suggest that dysregulation of the complement system plays a role in microglia-mediated spine loss. This mechanism, known to be involved in the removal of redundant synapses during development, is likely reactivated in Type II FCD, particularly in Type IIb; local treatment with anticomplement drugs could in principle modify the course of disease in these patients.

## KEYWORDS

complement, dendritic spine, epilepsy, focal cortical dysplasia, microglia, organotypic culture

This is an open access article under the terms of the [Creative Commons Attribution-NonCommercial-NoDerivs](https://creativecommons.org/licenses/by-nc-nd/4.0/) License, which permits use and distribution in any medium, provided the original work is properly cited, the use is non-commercial and no modifications or adaptations are made.

© 2022 The Authors. *Brain Pathology* published by John Wiley & Sons Ltd on behalf of International Society of Neuropathology.

## 1 | INTRODUCTION

Dendritic spines are the postsynaptic sites of synaptic exchange in the mammalian brain. They receive and integrate the majority of excitatory synaptic inputs and directly influence neuronal excitability in physiological and pathological conditions [1,2]. Numerous neurological brain diseases are associated with abnormalities in morphology and density of dendritic spines, such as Alzheimer disease (AD), multiple sclerosis (MS), schizophrenia, and epilepsy, which indicates the importance of proper spine regulation [3,4]. In human epileptic tissues, spine loss and dendritic abnormalities are most consistently reported in hippocampi from patients with intractable temporal lobe epilepsy (TLE) [5,6], while fewer and partly conflicting data are available for neocortical tissue samples because of the different etiological substrates considered in the different cohorts [7–10]. Establishing whether dendritic spine pathologies are a cause or consequence of epilepsy is still an open question; still, their presence is suggested to be implicated in (i) epilepsy aggravation, (ii) promoting hyperexcitable circuits and seizures, and (iii) contributing to cognitive deficits [11,12]. Therefore, understanding the mechanisms leading to dendritic spine alterations is crucial and may help to identify novel strategies to treat or prevent seizures and the associated neurological comorbidities.

One of the mechanisms suggested for spine loss is linked to the discovery of an unexpected role for the classical complement cascade in the developmental elimination of extranumerary synapses, that is, synaptic pruning. Emerging data suggest that the classical complement pathway, a key part of the innate immune system, can guide microglia to phagocytose synapses. In particular, the initiator of the classical pathway, complement protein C1q, can serve as an “eat me” signal to promote phagocytosis from microglia [13,14]. This mechanism has been clearly demonstrated during normal brain development, where complement proteins are localized in developing central nervous system (CNS) synapses during the period of active synapse elimination; recently, it has been hypothesized that similar mechanisms could be reactivated in pathological conditions [13–17]. This assumption is supported by data showing abnormal reactivation of the complement cascade in several brain diseases, such as AD [18], MS [19], and schizophrenia [20], and in normal aging [14]. Moreover, a direct role for C1q protein in pathological synapse loss has been demonstrated in AD, where C1q protein accumulation in the postsynaptic densities is associated with augmented microglial engulfment of synapses and decline of synapse density [18].

In epilepsy, enhanced classical complement pathway activation was observed in several epileptic conditions, including mesial temporal sclerosis (MTS), tuberous sclerosis complex (TSC), and focal cortical dysplasia (FCD), as a part of an inflammatory state suggested to be involved in the process of epileptogenesis of these lesions

[21–24]. Our group recently utilized Golgi-Cox impregnation on postsurgical human tissue to demonstrate the presence of a severe dendritic pathology characterized by spine loss and synaptic alterations in Type II FCD, a developmental cortical malformation and frequent cause of drug-resistant epilepsy. Notably, these morphological alterations were not observed in adjacent perilesional areas or in other post-surgical epileptic tissue samples obtained from Type I FCD, TLE with hippocampal sclerosis, and nonlesional (cryptogenic) cases [10]. Based on these data, in this study, we investigated C1q/C3 expression and the presence of activated microglia cells in postsurgical neocortical specimens obtained in a well-characterized epilepsy patient cohort. These findings and the presence of dendritic spine loss were correlated to the different etiologies. In a separate set of experiments, we investigated the role of the complement components C1q and C3 as regulators of synaptic pruning using human *in vitro* slices and suggest that a dysregulation of the complement system in Type II FCD might promote microglia-mediated spine loss.

## 2 | MATERIALS AND METHODS

### 2.1 | Subjects

The study includes the analysis of postsurgical neocortical tissues from 20 subjects admitted to neurosurgery for drug-resistant epilepsy at the Fondazione Istituto Neurologico Carlo Besta or the Claudio Munari Epilepsy Surgery Center at Niguarda Hospital (Milan, Italy). All patients underwent surgery after a comprehensive electroclinical and Magnetic Resonance Imaging (MRI) evaluation. The resections were performed for strictly therapeutic reasons after the patients had given their informed consent, and the extent of the excision was planned preoperatively on the basis of the epileptogenic zone location (defined on the basis of anatomoelectroclinical data) and of the risk of postsurgical deficits. Seizure freedom was monitored periodically and was determined using Engel outcome scale [25]. Written informed consent was obtained for the use of brain surgical specimens and clinical data for research purposes, in compliance with institutional and national ethical guidelines, and the protocol for the study was approved by the local ethical committee.

Table 1 summarizes the main clinical data and the histopathological diagnosis: cryptogenic epilepsy (no lesion), TLE with hippocampal sclerosis with no alterations in the neocortex (TLE-hippocampal sclerosis [HS]) and FCD Type IIa/b. Figure 1 highlights the main histopathological features of the different cases. Table 2 lists the experiments performed for each group of samples. In particular, based on our published mercuric Golgi-Cox impregnation work [10], we had samples with well-characterized dendritic spine density (ID 1, 2, 4, 5, and 8–14) showing normal (Group 1) and reduced spine density (Group 2), respectively; for the validation

TABLE 1 Clinical data of the patients.

ID	Diagnosis	Age at epilepsy onset, y	Epilepsy duration, y	Age at surgery, y	Site of surgery	Outcome (Engel class)
1	Cryptogenic	29	17	46	T	II
2	Cryptogenic	9	27	36	T	IIIA
3	Cryptogenic	30	12	42	T	IA
		<b>23 (12)</b>	<b>19 (8)</b>	<b>41 (5)</b>		
4	TLE-HS	7	28	35	T	IA
5	TLE-HS	10	30	40	T	IA
6	TLE-HS	19	38	57	T	II
7	TLE-HS	14	4	18	T	IA
		<b>14 (5)</b>	<b>24 (18)</b>	<b>38 (20)</b>		
8	FCD IIa	0	16	16	T	IA
9	FCD IIa	2	25	27	F	II
10	FCD IIa	4	6	10	F	IA
11	FCD IIb	7	15	22	F	IA
12	FCD IIb	11	17	28	F	IA
13	FCD IIb	3	49	52	F	IC
14	FCD IIb	9	33	42	F	IA
15	FCD IIb	1	33	34	F	IA
16	FCD IIb	8	38	46	F	II
17	FCD IIb	1	1	2	F	IA
18	FCD IIb	1	3	4	F	IA
19	FCD IIb	10	8	18	F	IA
20	FCD IIb	6	40	46	P	IA
		<b>5 (4)</b>	<b>22 (16)</b>	<b>27 (17)</b>		

Note: Means  $\pm$  SD are indicated in bold for each diagnostic category.

Abbreviations: F, frontal; FCD, focal cortical dysplasia; ID, identification number; P, parietal; T, temporal; TLE-HS, temporal lobe epilepsy with hippocampal sclerosis; y, year.

of the immunohistological findings, we included an additional cohort of Type IIb FCD cases (ID 15–20); for functional in vitro studies, utilizing organotypic cultures, we added further three cases (ID 3, 6, and 7).

## 2.2 | Immunohistochemistry and confocal microscopy

After surgery, *en bloc* resected brain specimens were immediately immersed in fixative solution (4% paraformaldehyde [PFA]) for 24–36 h, excepting the fresh slabs immersed in the Golgi-Cox solution for dendritic spine evaluation [10] or used for organotypic culture (see below). After fixation, the tissues were embedded in paraffin and, in some cases, partly destined to be cut by a vibratome (VT1000S, Leica). For routine neuropathology, serial 7- $\mu$ m thick paraffin sections were stained with hematoxylin and eosin, thionin, and Klüver–Barrera stain. For the diagnosis, each case was processed for immunohistochemistry using monoclonal antibodies against neuron-specific nuclear proteins (NeuN, Millipore, Temecula, California, 1:1000) to evaluate cortical lamination and neuronal density, neuronal nonphosphorylated neurofilaments (SMI311R; Covance, San Diego, California, 1:250) and

microtubule-associated protein (MAP2; NeoMarkers, Fremont, California, 1:100) as markers of dysmorphic neurons (DNs), glial-fibrillary acidic protein (GFAP; Millipore, 1:1000) for astrogliosis, and intermediate filament protein vimentin (Dako, Carpinteria, California, 1:1000) as marker for balloon cells (BCs). For the specific purpose of this study, additional sections were immunoreacted using monoclonal antibodies against the complement proteins C1q (9H10, IgG2b, 95  $\mu$ g/ml) and C3 (C3.30, which binds to C3b, iC3b, and C3c activated fragments, IgG1, 12  $\mu$ g/ml) both kindly provided by Prof. Morgan [26]; polyclonal antibody against ionized calcium-binding adaptor molecule 1 (Iba1, Abcam, Cambridge, UK, 1:300) as microglia marker and monoclonal antibody against human leukocyte antigen class II (HLA-DP/DQ/DR, clone CR3/43, Dako, 1:200) as a marker of activated microglia. Single-label immunohistochemistry was developed using avidin-biotin-peroxidase method with 3,3-diaminobenzidine (DAB, Sigma, St Louis, Missouri) as chromogen, on sections counterstained with hematoxylin. To control the specificity of primary antibodies, sections were stained according to standard protocol except for the primary antibody incubation step, which was omitted. No immunostaining was ever observed under this condition.

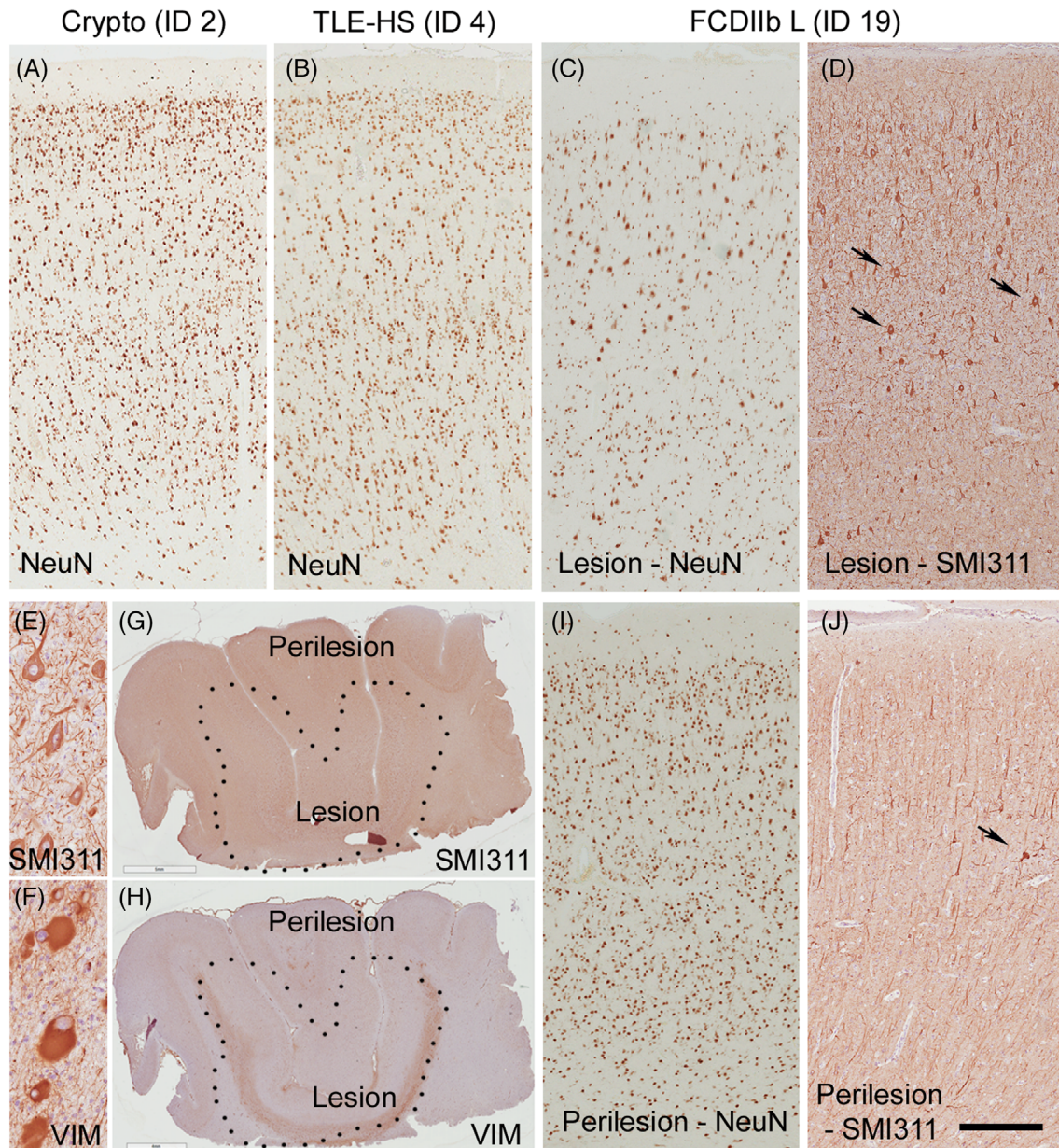


**FIGURE 1** Representative histological features in cortical samples from patients with different histological diagnosis. (A,B) Neuronal nuclei (NeuN) immunoreactivity (ir) in cryptogenic and temporal lobe epilepsy with hippocampal sclerosis (TLE-HS) cases, respectively. Both are characterized by a normal cortical laminar organization. (C–J) Different ir in a case of Type IIB focal cortical dysplasia (FCD) showing the presence of cortical dyslamination, reduced cellular density (C; NeuN-ir), numerous dysmorphic neurons [DNs] (D,E; SMI311-ir, arrows in D) and balloon cells (BCs; F, vimentin-ir). (G,H) Low magnification of SMI311- and vimentin-ir; the core of the lesion (L) and the adjacent perilesional area (P) are indicated. (I,J) In the perilesional area, only rare and scattered DNs (arrow in J) are visible (NeuN-ir and SMI311-ir, respectively). Scale bar: 430  $\mu$ m (A–D,I,J), 75  $\mu$ m (E,F), and 5.6 mm (G,H)

Representative paraffin or vibratome sections were used for double immunofluorescence labeling. The sections were incubated in a mixture of antibodies against C1q/GFAP, C1q/Iba1, C3-fragments/GFAP, C3-fragments/Iba1 (FCD II cases), or MAP2/Iba1 (FCD II/cryptogenic), followed by appropriate indocarbocyanine (Cy) 2-conjugated goat anti-mouse and (Cy) 3-conjugated goat anti-rabbit antibodies. The sections were then observed using a TCS SP8 AOBS laser-scanning confocal microscope (Leica Microsystems). The same cases were also used for double-labeled

immunohistochemistry combining MAP2/Iba1. The different peroxidase substrates allowed for simultaneous visualization of the two antigens.

### 2.3 | RNA scope for C1q mRNA

RNA in situ hybridization technology (RNAscope) was applied to map C1q RNA expression in 5- $\mu$ m thick paraffin sections in representative cases. Briefly, tissue

TABLE 2 Experiments performed for each group of samples.

	ID	Diagnosis	Experiments performed
GROUP 1: normal spine density	1	Cryptogenic	Golgi and dendritic spine evaluation
	2	Cryptogenic	IHC (C1q, C3, Iba1, and HLA-DR)
	4	TLE-HS	C1q RNAscope
	5	TLE-HS	
	8	FCD IIa	
	9	FCD IIa*	
	8–14	FCD perilesions	
Group 2: reduced spine density	10	FCD IIa	Golgi and dendritic spine evaluation
	11	FCD IIb	IHC (C1q, C3, Iba1, and HLA-DR)
	12	FCD IIb	C1q RNAscope
	13	FCD IIb*	
	14	FCD IIb*	
	15	FCD IIb	IHC (C1q, C3, Iba1, and HLA-DR)
	16	FCD IIb	C1q RNAscope
	17	FCD IIb	
	18	FCD IIb	
	19	FCD IIb	
	20	FCD IIb	in vitro slices, C1q-C3 treatment,
	3	Cryptogenic	DiI staining
	6	TLE-HS	
	7	TLE-HS	

Note: \*Indicates cases in which the dendritic spine evaluation on Golgi staining is only qualitative.

Abbreviations: DiI, 1,1'-diiodo-3,3',3'-tetramethylindocarbocyanine perchlorate; FCD, focal cortical dysplasia; ID, identification number; IHC, immunohistochemistry; TLE-HS, temporal lobe epilepsy with hippocampal sclerosis.

sections were incubated in Target retrieval reagent for 15 min at 100°C, followed by protease treatment (10 µg/ml protease PLUS) at 40°C for 30 min in a HyBEZ hybridization oven (RNAscope® 2.5 Reagent Kit, Advanced Cell Diagnostics, Biotechne, California). RNAscope® Probe Hs-C1QA (Biotechne) was then hybridized for 2 h at 40°C followed by RNAscope amplification and fast red chromogenic detection. The endogenous housekeeping gene UBC as positive control and the bacterial gene *dapB* as negative control (Biotechne) were hybridized to assess tissue RNA integrity, assay procedure, and background signals. Moreover, using a fluorescent dye it was possible to combine C1QA probe detection with Iba1 and GFAP immunofluorescent analysis or Nissl staining following the manufacturer protocol.

## 2.4 | Quantification of complement proteins and microglia expression

Quantitative evaluation of C1q, C3, Iba1, and HLA-DR was performed on immunoreacted paraffin tissue sections in all cases (Table 2). Briefly, in one section per case representative of the histopathology, two regions of interest (ROIs) in the gray matter (total 0.36 mm<sup>2</sup>) and two in the white matter

(0.36 mm<sup>2</sup>) were acquired at 20× magnification with a Nikon digital camera. The ROIs were selected based on the most prominent staining as a rule and, in Type II FCD cases, in regions containing the maximum dysplastic alterations (named Lesion, L) and in adjacent normal-appearing cortex (Perilesion, P, when present). After quenching hamatoxylin signal and gray conversion using the Image-Pro Premiere 9.1 software (Media Cybernetics, Silver Springs, Maryland), quantification of immunohistochemistry was performed using field fraction analysis. Field fraction is a method that gives an accurate estimation of the percentage of immunostaining within an area of interest using a threshold mask set to maximize recognition of the staining and keep constant among the different images.<sup>27</sup> Data were expressed as percentage of immunostaining (field fraction) within the area of interest and changes (i) among the different histopathological entities (all cases) or (ii) between cases with normal or reduced spine density (Groups 1 and 2, Table 2) were then evaluated.

## 2.5 | Transmission electron microscope

In one Type IIb FCD case, part of the specimen after 4% PFA fixation was cut at serial 50 µm-thick sections

using a vibratome (VT1000S, Leica Microsystems, Heidelberg, Germany) and processed for pre-embedding immunohistochemistry. Vibratome sections underwent mild ethanol pretreatment to increase the penetration of immunoreagents, and were processed with the immunoperoxidase protocol to detect Iba1 immunoreactivity (1:1000 in blocking solution). The immunoreacted section was then postfixed for 10 min in 2.5% glutaraldehyde in PB, washed and postfixed for 1 h in 1% OsO<sub>4</sub>, dehydrated, cleared in propylene oxide, flat-embedded in Epon-Spurr between acetate sheets (Aclar; Ted Pella, Redding, California) and polymerized at 60° for 36 h. After polymerization, embedded sections were examined under a dissecting microscope and small gray matter areas inside the dysplastic lesion were excised with razor blades and glued to cured resin blocks. Semithin (1- $\mu$ m thick) sections were then cut with a ultramicrotome (Reichert–Jung Ultracut E, Germany) and collected on glass slides with toluidine blue counterstaining for light microscopic inspection to control the histopathological features. In areas of interest, ultrathin sections (80 nm) were then obtained, counterstained with lead citrate and samarium and gadolinium triacetate and examined with a Tecnai™ Spirit transmission electron microscope.

## 2.6 | Organotypic cultures

### 2.6.1 | Slice preparation and incubation

Slices for organotypic culture were prepared from three surgical cases (ID 3,6,7, Table 2). Five-millimeter thick slabs were excised from the neocortical tissues in the operating room, immediately placed in ACSF solution containing (in mM): NaCl, 87; NaHCO<sub>3</sub>, 26; NaH<sub>2</sub>PO<sub>4</sub>, 1.2; KCL, 2.5; CaCl<sub>2</sub>, 0.5; MgCl<sub>2</sub> 10; sucrose, 75 and D-glucose, 25 (all from Sigma-Aldrich, St. Louis, Missouri), at 2°C–10°C, gassed with 95% O<sub>2</sub>/5% CO<sub>2</sub>, adjusted to 305–315 mOsm, pH 7.4 and immediately transported to the laboratory. Maintaining the orientation, the tissue was glued onto the cutting platform and 300- $\mu$ m thick coronal slices were cut with a vibratome (VT12005, Leica Microsystems) in ice-cold ACSF continuously bubbled with 95% O<sub>2</sub> and 5% CO<sub>2</sub>. After cutting, slices were washed for 15 min in a solution of Hanks' balanced salt solution with added hydroxyethylpiperazine ethane sulfonic acid (HEPES) (20 mM; room temperature, gassed with 95% O<sub>2</sub>/5% CO<sub>2</sub>, pH 7.3, osmolarity 305–315 mOsm). Slices were then placed on membranes of an insert in a 6-well plate (30 mm Transwell, Merck-Millipore, Burlington, USA) and 1 ml of culture medium was placed in each well. The medium composition was: Neurobasal (Gibco, Paisley, UK) supplemented with 2% serum-free B-27 (Gibco), 2% Pen/Strep, 13 mM D-glucose (Sigma-Aldrich), 1 mM MgSO<sub>4</sub> (Sigma-Aldrich), 15 mM

HEPES (Sigma-Aldrich), 2 mM GlutaMAX (Gibco), 0.25  $\mu$ g/ml Amphotericin B (Gibco). When the 6-well culture plates were transferred to an incubator, slices were maintained at an interface between the medium and a 5% CO<sub>2</sub> in air atmosphere at 37°C.<sup>28</sup> The medium was changed daily.

### 2.6.2 | Slice treatments and fluorescent tracer application

For complement protein treatment, 24 h after the slice preparation ( $t = 24$  h), the medium was supplemented with 1 ng/ml C1q or 1 ng/ml each of C1q and C3 (HyCultBiotech, Uden, The Netherlands) and maintained for 1 or 2 days. Slices were collected ( $t = 48$  or 72 h) on a glass slide, crystals of 1,1'-dioctadecyl-3,3,3',3'-tetramethylindocarbocyanine perchlorate (DiI, Invitrogen, Massachusetts) were placed in the middle of the cortical gray matter using a bamboo fiber under a dissecting microscope, and conserved in a dark room for a further 24 h to allow the diffusion of the dye and the visualization of dendritic segments and dendritic spines. The slices were then rinsed in PB, fixed in 4% PFA for 30 min, mounted with FluorSave™ and examined with a confocal microscope (TCS SP8 AOBS, Leica microsystem). At  $t = 48$  and 72 h, some slices were fixed in 4% PFA and used as immunohistochemical controls to assay the viability using MAP2 and NeuN immunohistochemistry. Cultured slices without complement protein treatment (named not treated) and not cultured slices immediately labeled with DiI (named baseline) were used as internal controls (see Figure 6A for a schematic drawing of the protocol). Unfortunately, not every treatment/time point was verified for each case depending on tissue availability or technical problems (see Table S2 for all the details).

### 2.6.3 | Confocal imaging, reconstruction, and analysis

Confocal images at different treatments and time points were acquired with a PLANAPO 63x/1.4 NA oil immersion objective by using a TCS SP8 AOBS laser-scanning confocal microscope (Leica Microsystem) equipped with an Ar/Ar-Kr 488, 561, and 633 nm diode laser lines and Hybrid detectors. The parameters for acquisition (561 laser line power and Hybrid detector gain) were defined on control conditions and kept constant for all the samples. For the acquisition, we focused on areas where DiI diffused and dendritic spines were clearly visible. Every image included dendritic segments (from 2 to 7) characterized by medium and small thickness, equally represented in the analysis, suggestive of proximal and distal ramifications. The 3D reconstruction of DiI-filled dendrites was performed using the Simple Neurite Tracer, a dedicated module of Fiji software, and the total

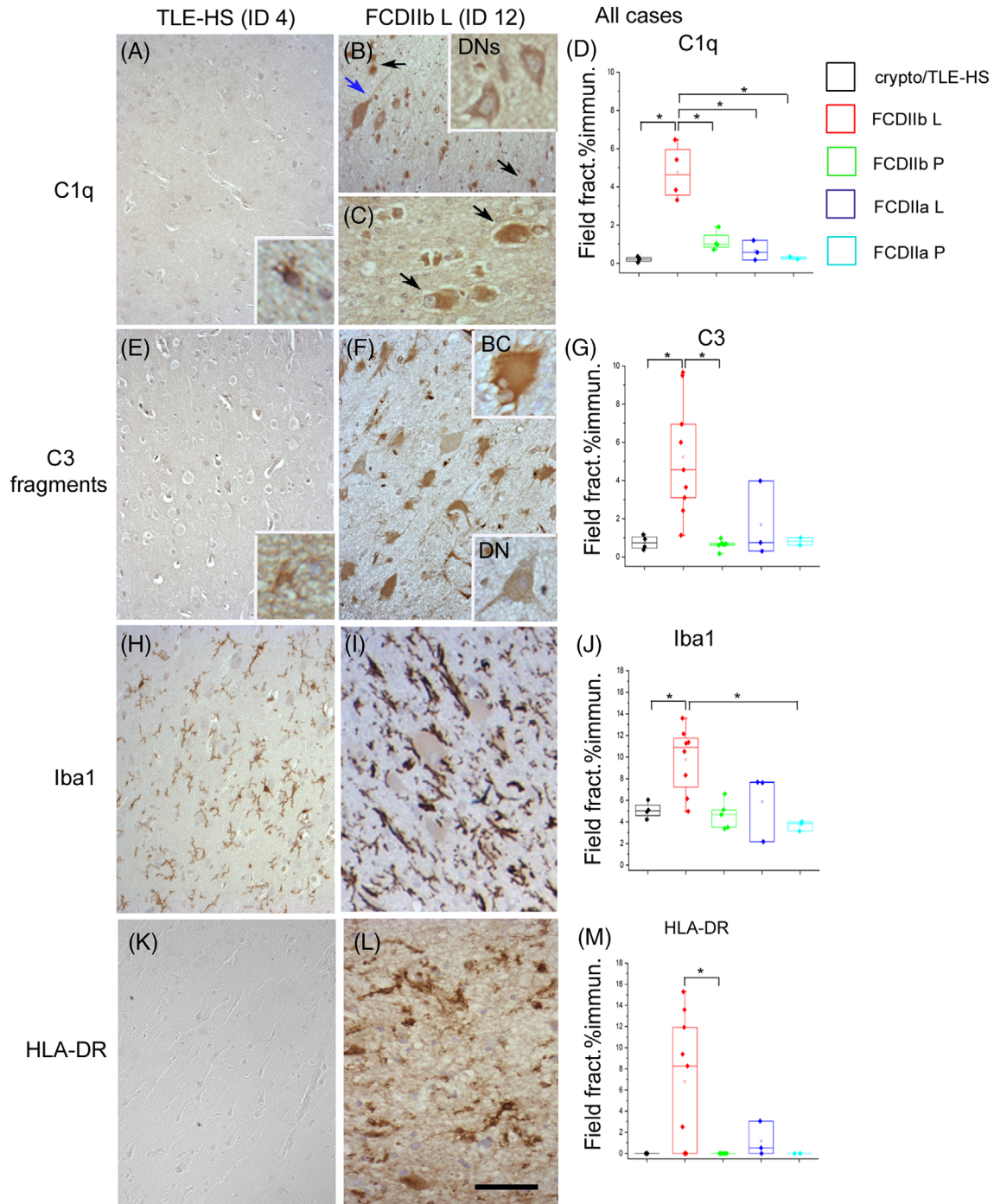


**FIGURE 2** Enhanced activation of the complement system and microglia reactivity in Type IIb focal cortical dysplasia (FCD) cases. Immunohistochemical evaluation of C1q (A,B,C), C3 fragments (E,F), Iba1 (H,I), human leukocyte antigen (HLA)-DR (K,L), and corresponding quantification (D,G,J,M) performed in all cases. Note that the low levels of C1q protein and C3-fragments in a temporal lobe epilepsy with hippocampal sclerosis (TLE-HS) case (A,E), with only scattered positive astrocytes in white matter (insets) in contrast to the increased level in Type IIb FCD lesion with high expression of both complement proteins in astrocytes, dysmorphic neurons (DNs) and balloon cells (BCs; B,C,F). No evident C1q/C3-fragments positive microglial cells are observed in the different cases. Microglial reactivity, evaluated with Iba1/HLA-DR markers of microglia/activated microglia, is also enhanced in Type IIb FCD lesion (I,L) in comparison to cryptogenic (H,K). (D,G,J,M) Quantification of the immunohistochemical data confirm the higher levels of complement proteins (C1q, C3) and microglial markers (Iba1, HLA-DR) in FCD IIb lesional area (L) in comparison to crypto/TLE-HS/FCD IIa cases and perilesional area (P) of FCD. HLA-DR immunoreactivity showed high variability. Asterisks indicate statistical significance ( $*p < 0.05$ ). Scale bar: 100  $\mu$ m (A–C,E,F), 60  $\mu$ m (insets in A,B,F,H,I,K,L).

dendrite length was measured. The number of dendritic spines was evaluated using the ImageJ program (<http://imagej.nih.gov/ij/>) and the spine density was then

calculated. Mean spine density changes at 48/72 h after the two different treatments were calculated (control values set to 1).

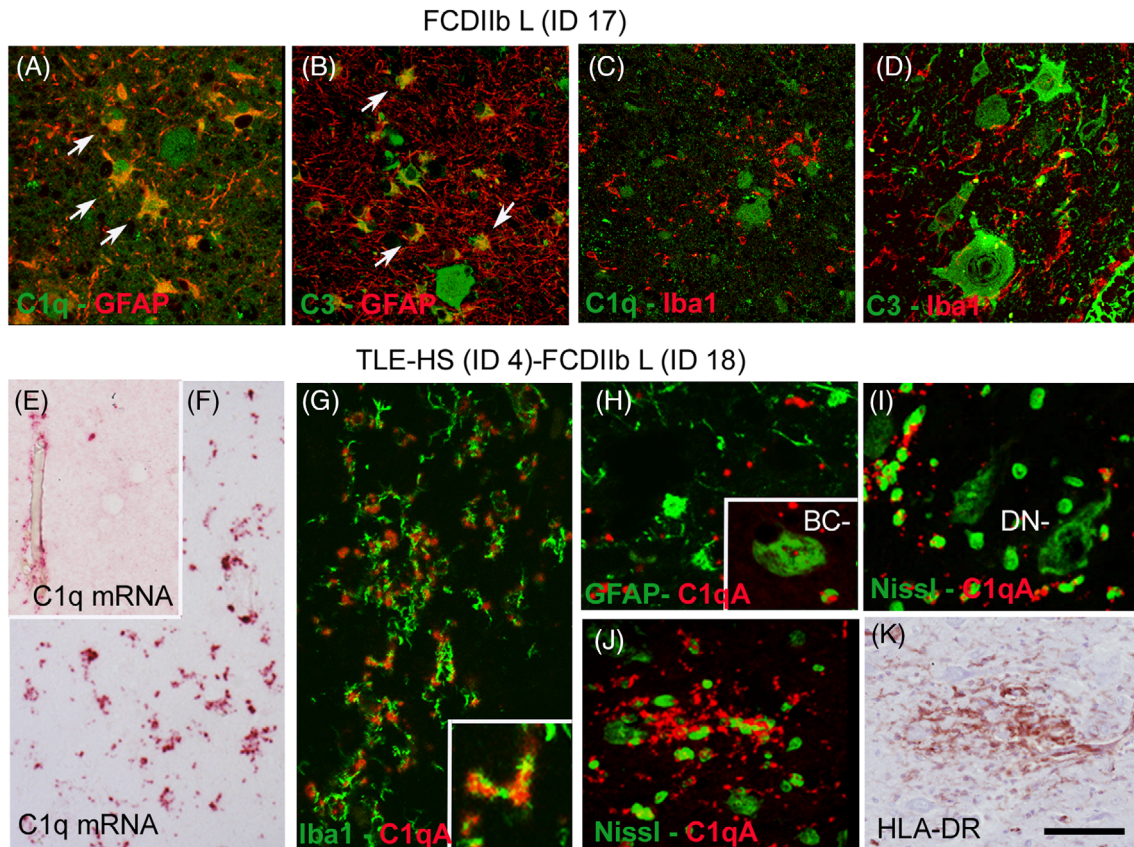


**FIGURE 3** Complement proteins localization and increased mRNA expression in Type IIb focal cortical dysplasia (FCD) cases. (A–D) Double immunofluorescence demonstrates the presence of C1q and C3-fragments in astrocytes (A,B) but not in microglia (C,D) in Type IIb FCD. (E–J) In situ hybridization detects higher C1qA mRNA expression, visualized as punctate dots, in Type IIb FCD (F) in comparison to cryptogenic/temporal lobe epilepsy with hippocampal sclerosis (TLE-HS) cases (E; showing the ID 4 case). C1QA probe detection combined with immunofluorescent analysis or Nissl staining, showing C1q mRNA co-localizing with microglia (G) but not with astrocytes, balloon cells (BCs, H) and dysmorphic neurons (DNs, I). Clusters of C1qA mRNA (J) in correspondence with clusters of activated microglia in Type IIb FCD cortex (K). Scale bar: 60  $\mu$ m (A–D,H; inset in H), 30  $\mu$ m (G), 20  $\mu$ m (inset in L), 50  $\mu$ m (I,J), and 90  $\mu$ m (K). HLA, human leukocyte antigen

## 2.7 | Statistical analysis

Differences in the histological measurements (C1q, C3, Iba1, and HLA-DR immunohistochemistry) among histological categories were evaluated with one-way analysis of variance (ANOVA) test followed by individual post hoc comparison using Tukey's test, while between the two subgroups (Groups 1 and 2) by two-sample *t*-test. A *p*-value of  $<0.05$  was considered significant. The Shapiro–Wilk normality test was used to prove normal data distribution. Correlation between spine density values and immunohistochemistry was tested with Pearson's test. Statistical analysis was performed using Origin 8.0 software.

## 3 | RESULTS

All the patients included in this study had a history of drug-resistant epilepsy and, most of them were adults at time of surgery (mean age was 31 years, range = 2–57). Postoperatively, 75% of patients were completely seizure-free (Engel

Class IA, Table 1). Representative histological features of the different cases are shown in Figure 1. Neocortical samples from patients with cryptogenic epilepsy or TLE-HS were characterized by normal cortical layering and no cellular abnormalities (Figure 1A,B), while in the Type II FCD cases, severe laminar disorganization and reduced cellular density were evident in the core of the lesion (Figure 1C,D). The presence of abnormal cells, such as giant DN or DN with BCs (Figure 1D–F), were cardinal signs of types IIa and IIb FCD, respectively. Normal-appearing cortex (Figure 1G–J), called perilesion, was present in most Type II FCD cases and was considered as an internal control for quantitative measurements. No sign of hippocampal sclerosis was present in the only temporal FCD IIa case.

### 3.1 | Enhanced expression of the complement system and microglial reactivity in Type IIb FCD cases

In cryptogenic/TLE-HS cases, low levels of C1q protein and C3 activation fragments were observed with



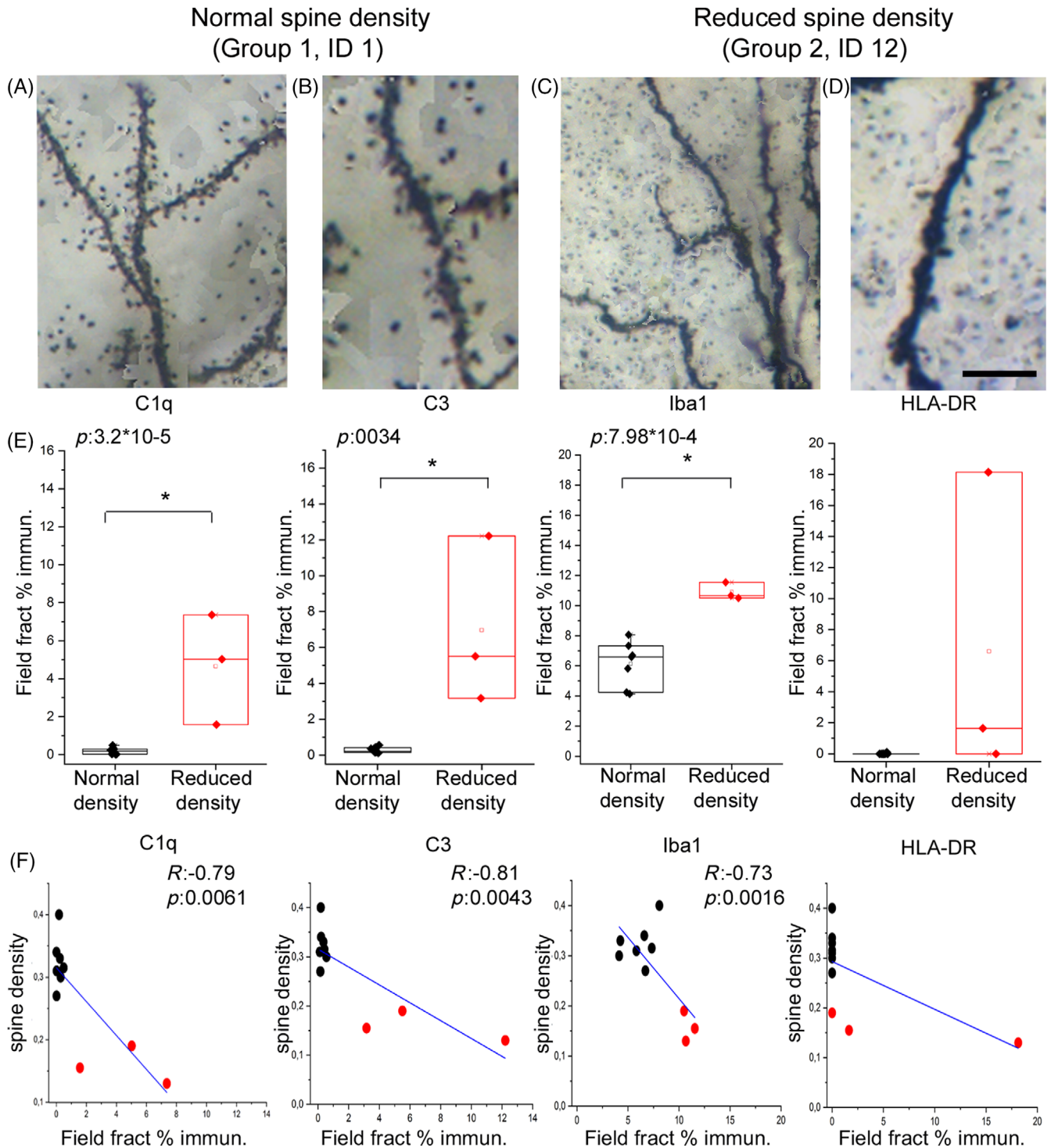


**FIGURE 4** Relationship between dendritic spine density and complement/microglial levels. Examples of Golgi-impregnated dendritic segments in cases with normal spine density (A,B; Group 1, the images are referred to a cryptogenic case) or reduced spine density (C,D; Group 2, images from a Type IIb focal cortical dysplasia [FCD] case). (E) Box plots showing re-evaluation of the previous C1q, C3, Iba1, and human leukocyte antigen (HLA)-DR immunohistochemical data considering only cases with spine density quantification. Note that the increase of complement and microglial proteins in cases with spine density reduction; HLA-DR showed variability (asterisks indicate statistical significance,  $p < 0.05$ ). (F) Graphics showing that spine density values negatively correlated with the levels of C1q, C3-fragments, Iba1 (Person correlation,  $p < 0.05$ ). Black dots represent cases with normal spine density (Group 1), whereas red dots are cases with reduced spine density (Group 2). Scale bar: 30  $\mu\text{m}$  (A,C) and 15  $\mu\text{m}$  (B,D).

immunohistochemistry in scattered white matter astrocytes (Figure 2A,E). By contrast, increased level was consistently observed in the core of Type IIb FCD with high

expression of both proteins in astrocytes, BCs and in a proportion of DNPs in gray and white matter (Figure 2B,C,F). No C1q/C3-fragments-positive

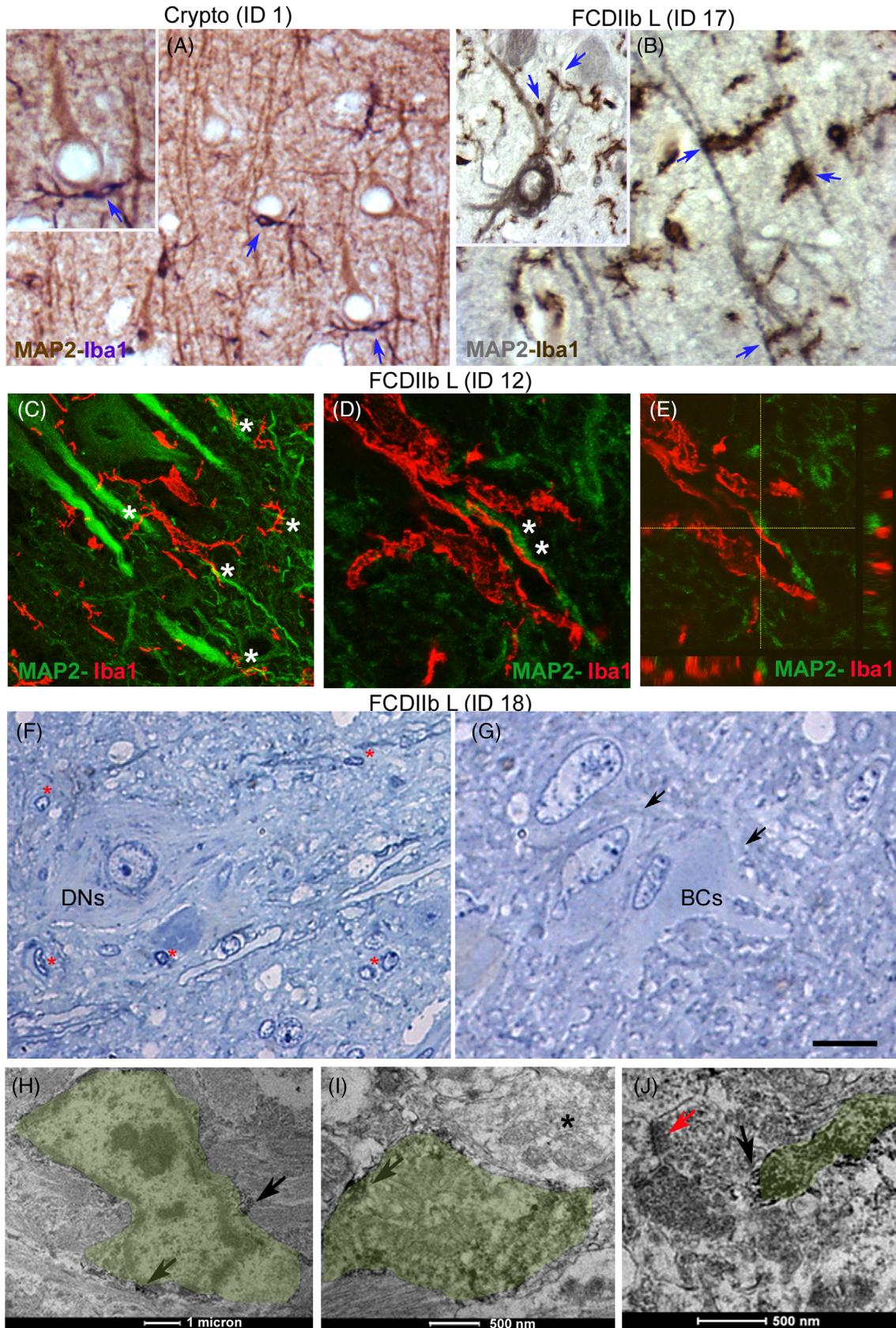


FIGURE 5 Legend on next page.

microglial cells were observed. Increased number of Iba1-positive and HLA-DR-positive microglial cells was detected in FCD IIb cases in comparison to the other groups (Figure 2H,I,K,L). In FCD Type IIa, results were conflicting with only one of three cases showing moderate increased levels of these markers (ID = 10, data not shown). Quantification of the immunohistochemical data performed on the entire cohort confirmed the higher levels of complement proteins (C1q, C3) and microglial markers (Iba1, HLA-DR) in FCD IIb core of the lesion (FCD IIb-L) in comparison to crypto/TLE-HS, FCD IIa cases and perilesional FCD areas (FCD IIb-P and FCD IIa-P); HLA-DR immunoreactivity showed high variability (Figure 2D,G,J,M).

### 3.2 | Complement proteins localization and increased mRNA expression in Type IIb FCD cases

Double labeling experiments in Type IIb FCD cases confirmed the prominent C1q/C3 presence in astrocytes (Figure 3A,B) and the lack of visible complement immunoreactivity in microglial cells (Figure 3C,D). C1q mRNA expression was low in cryptogenic/TLE-HS cases, predominantly localized around vessels (Figure 3E), while it was augmented in FCD IIb cases (Figure 3F), in agreement with immunohistochemistry. Combining C1qA probe detection with double immunofluorescence analysis or Nissl staining indicated that the gene was mainly expressed in Iba1-positive microglial cells but not in astrocytes, BCs, or DNs (Figure 3G–J).

### 3.3 | Relationship between dendritic spine density and complement/microglial levels

Based on a previous quantitative analysis of spine density [10], we identified cases with normal spine density (Group 1 composed of crypto, TLE-HS, two Type IIa FCD and all the perilesional area of FCD, Table 2) and reduced spine density (Group 2 composed of Type IIb and one IIa FCD, Table 2). Examples of Golgi-impregnated dendritic

segments and spine density in both groups are shown in Figure 4A–D. We next re-evaluated C1q, C3, Iba1, and HLA-DR immunohistochemical data obtained in gray matter considering only cases with quantified spine density and statistical analysis highlighted the significant increase of C1q, C3-fragments, and Iba1 protein staining in cases with spine density reduction; HLA-DR showed high variability (Figure 4E). Moreover, spine density value negatively correlated with the level of C1q, C3-fragments, and Iba1 (Person correlation,  $p < 0,05$ , Figure 4F). These data suggest a relationship between the loss of spine density observed in gray matter of FCD II cases and complement/microglial activation.

### 3.4 | Microglia recruitment on dendritic arbor in tissues affected by spine loss

Double colorimetric immunohistochemistry combining the neuronal marker MAP2 with Iba1 showed the different spatial localization of Iba1-positive microglial cells in cases with either normal or reduced spine density. In the normal spine density group (Group 1), microglia were prevalently observed around the soma of pyramidal neurons only occasionally contacting dendrites (Figure 5A). In cases with decreased spine density (Group 2), microglia with activated morphological features were frequently observed in contact with dendritic segments (Figure 5B). Microglia–dendritic interactions in Type IIb FCD cases were further confirmed using confocal microscopy (Figure 5C–E and Figure S1) and electron microscopy. Immunohistochemical electron microscope for Iba1 was performed in one case of FCD IIb and a small gray matter region in the lesional core was analyzed. An 1- $\mu\text{m}$  thick semithin sections showed the presence of DN, surrounded by numerous glial nuclei and BCs with pale opalescent cytoplasm and eccentric nuclei (Figure 5F,G). The same region, cut at 80 nm and observed at ultrastructural level, showed microglial cells and microglial processes, identified by the presence of DAB-positive electron-dense Iba1 immunolabeling in the cytoplasm, contacting dendritic shaft and sometimes in close proximity to synaptic profile (Figure 5H–J).

**FIGURE 5** Microglial recruitment on dendritic arbor in cases with spine loss. (A,B) Double colorimetric ir combining the neuronal marker MAP2 with Iba1 microglial marker in cases with normal or reduced spine density. In the first group, Iba1-positive cells are frequently localized around the soma and rarely contact dendrites (A and inset, blue arrows). In contrast, in the second group, numerous Iba1-positive cells, with activated morphological features, are frequently in contact with dendritic segments (B and inset, blue arrows). (C,D) z stack confocal projections suggesting multiple contacts (asterisks) between MAP2-positive dendrites and activated Iba1-positive microglia. In (E), a single focal plane extracted from (D) clearly demonstrates juxtaposition between the two structures in the three different planes (cross-hair). (F–J) Representative images obtained from a Type IIb focal cortical dysplasia (FCD) case immunoreacted for Iba1 and processed for electron microscope. (F,G) One-micron semithin section counterstained with toluidine blue showing a large DN surrounded by numerous glial nuclei (F, red asterisks) and BCs, with pale opalescent cytoplasm and eccentric nuclei (G, black arrows), typical sign of the FCD core of the lesion. (H–J) Electron micrographs of the same region represented in (F,G) showing a microglial cell (H, pseudo-colored in green) well identified according to morphological features and Iba1 electron-dense immunoreaction product in the cytoplasm (black arrows) and microglial processes contacting dendritic shaft (I, asterisk indicates the dendritic shaft) or in close proximity to synaptic profiles (J, red arrow indicates the synaptic strip). Scale bar: 24  $\mu\text{m}$  (A,B), 15  $\mu\text{m}$  (insets in A,B), 20  $\mu\text{m}$  (C), 10  $\mu\text{m}$  (D,E), and 10  $\mu\text{m}$  (F,G).

### 3.5 | Effect of complement proteins on dendritic spines in culture slices

Organotypic cultures prepared from three surgically resected brain samples (Table 2) were maintained 3 days *in vitro*. Adjacent tissue slabs did not show any sign of FCD on histological examination (data not shown). MAP2 and NeuN immunohistochemistry, performed at different time points and under different conditions, demonstrated good cell viability in culture slices in comparison to freshly cut slices used as baseline control. MAP2 immunoreactivity was present in the soma and proximal dendrites in numerous pyramidal neurons in all cortical layers (Figure 6B–D); tortuous apical dendrites, sporadically observed at 48 h *in vitro*, were not found at  $t = 72$  h. DiI crystals were used to visualize and quantify dendritic spines. Qualitative and quantitative data at baseline condition and at different time points in culture slices not receiving any treatment showed dendritic spines regularly distributed along the dendrites (Figure 6E,F) with homogeneous and comparable spine density (Table S1). Spines in cultured slices were more elongated (Figure 6F) compared with baseline tissue. In culture slices treated with C1q alone or C1q/C3 proteins for 48/72 h we observed a less homogeneous distribution along the dendritic segments with area devoid of dendritic spine (Figure 6G,H) and, in comparison to controls, a tendency of a reduction in spine density (Figure 6I and Table S1). The low number of analyzed cases did not allow a statistical analysis.

## 4 | DISCUSSION

A growing body of evidence supports the concept of a strict connection between inflammation and the presence of injured/altered brain tissue in epileptic patients. This relationship seems to be particularly strong in some epileptogenic cortical malformations, such as Type II FCD and TSC, both linked to mammalian target of rapamycin (mTOR) pathway dysregulation; in these focal epilepsies, neuronal loss, gliosis, white matter alteration, and dendritic spine loss are documented as well as the presence of neuroinflammation [10,29–32]. Starting from our previous data showing a severe dendritic spine loss in the core of human Type II FCD lesion [10], we have now extended the investigation on the potential contribution of complement and microglia in this dendritic pathology. The main findings of the present study are that (i) FCD Type II tissue samples, mainly Type IIb, presenting dendritic spine loss show a prominent activation of both the classical complement pathway and microglia, (ii) in the same cases, a close relationship between microglial cells and dendritic segments/synapses can be found, and (iii) noFCD human *in vitro* slices treated with complement proteins show a tendency to reduce

dendritic spine density. Altogether these data suggest that a complement-microglia-mediated reactivation of synaptic pruning might play a role in the dendritic spine loss observed in Type II FCD.

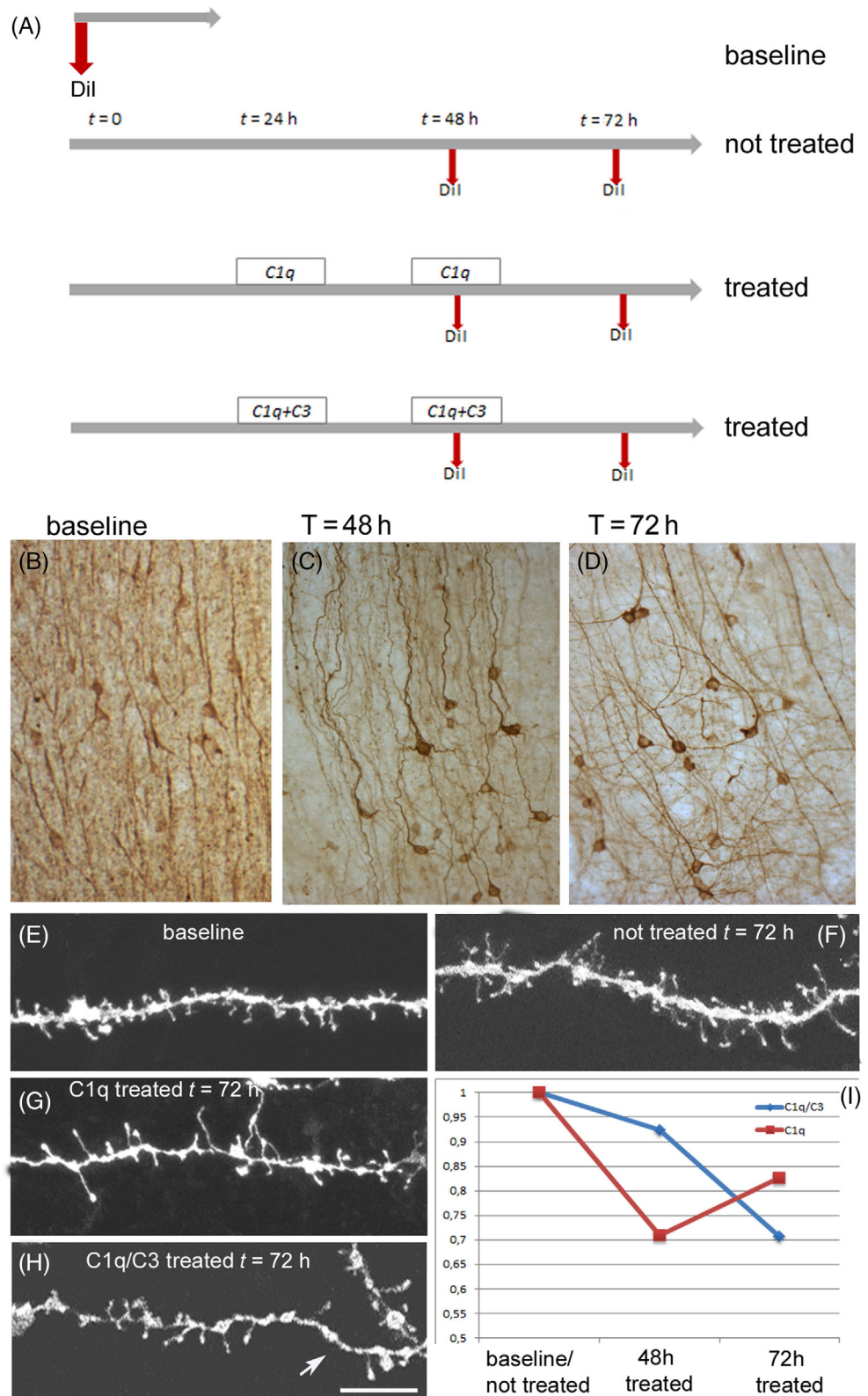
The presence of an upregulation of the classical complement pathway in human epileptic tissues, and particularly in Type IIb FCD, is supported by several other studies performed on postsurgical brain tissue [23,24,33,34]. Immunohistochemical data frequently report high level of complement proteins in astrocytes and in the abnormal DN and BCs. We confirm these data and demonstrate that C1q and C3b, iC3b, C3c activated fragments are detectable within the malformed area, particularly in Type IIb FCD, but are not observed in the perilesional tissue adjacent to the FCD core or in other epileptic tissues, such as cryptogenic epilepsy and TLE-HS, all patients presenting a long epilepsy history. These data further support the notion that an activation of inflammatory molecules is an intrinsic specific feature of this type of FCD and is not triggered by chronic seizure activity *per se* [29]. The discrepancy between the two FCD subtypes, with stronger expression of complement components in Type IIb than in IIa, also observed in a previous paper [34], is not an unexpected finding because they are different in several clinical, radiological, postsurgical outcome [35], and morphological aspects [29]. As suggested by Zimmer et al [34], BCs, the immature abnormal cells only present in Type IIb FCD, may be crucial driver of inflammation and partly explain the less severe alterations noted in IIa FCD. Wyatt et al. [23] also investigated the complement expression in neocortical tissues from patients with MTS and observed an increase of C1q and C3 proteins. The discrepancy with our data could be due to the different case selection, may be the presence of an associated dysplastic lesion in the neocortex (FCDIIIa), or to the different techniques (immunoblotting versus immunohistochemistry).

Using RNAscope technology, we identified microglia as the principal cell responsible for C1qA mRNA synthesis in epileptic tissues, confirming the local synthesis of this protein; however, we cannot exclude possible permeation of complement proteins from circulating blood. The detection of complement proteins in the other cells, such as DN, BCs, and astrocytes, but not the mRNA might be due to possible deposition or accumulation mechanism of C1q and C3 fragments on these cells.

Classical complement pathway is active in CNS during development, where it promotes proper synapse function and memory formation via removal of excess synapses [13]. Complement activation is reduced in early adulthood, but reactivation and dysregulation have been observed during aging and in neurodegenerative diseases; in these conditions, microglia, and astrocytes are the primary sources of the secreted complement proteins [14,16]. Our data, suggest a similar mechanism in Type II focal cortical malformation with microglia as the primary source for local complement production and deposition

**FIGURE 6** Effect of complement proteins on dendritic spines in culture slices.

(A) Schematic drawing of the different experimental treatments and time points. (B–D) MAP2 ir, in 300- $\mu$ m thick sections in different conditions: baseline (not cultured), after 48 or 72 h in culture without any complement treatment (not treated). In all conditions, we observe numerous immunolabeled pyramidal neurons, sign of cell vitality. (E–F) 3D reconstructions of Dil-filled dendrites in slices at baseline condition and after 72 h in culture without any treatment. Spines are regularly distributed along the dendrites in both conditions with a more elongated morphology in cultured slices. (G,H) After C1q and C1q/C3 treatments, spines are less numerous and irregularly distributed along the segments with empty areas (arrow in H). (I) Graphic representing the mean spine density changes at 48/72 h after the two different treatments (control values set to 1), note a tendency of spine reduction in both treatments in comparison to control. Scale bar: 80  $\mu$ m (B,D) and 20  $\mu$ m (E–H).



or phagocytose of complement proteins in the other cells (astrocytes and abnormal cells).

C1q and C3 proteins have recently emerged as key mediators of synaptic elimination by tagging synaptic connections for removal by phagocytic microglia, in both

physiological and pathological conditions [36]. Based on this evidence, we searched for a similar mechanism and analyzed the presence of microglia/activated microglia in our epileptic tissue samples. Microglia, the professional phagocytes of the CNS, are typically highly ramified with

dynamic processes that monitor the local environment. In epilepsy, they activate and develop an amoeboid morphology with short and thick processes [37]. As expected, immunohistochemistry in Type IIb FCD specimens revealed an increased expression level of Iba1-positive and HLA-DR-positive microglial cells with branched, hypertrophic morphology in comparison to control and other epileptic tissues.

The evaluation of the complement/microglial immunohistochemical data using exclusively samples with quantified dendritic spine changes showed significantly increased C1q/C3 levels coupled with microglial-dendritic contacts in tissues with reduced spine density (FCD IIb and 1 IIa cases) in comparison to tissues with normal spine density (crypto, TLE-HS, FCD IIa, and all the perilesional control tissue). Despite the limited number of cases, these data suggest a strict relationship between spine loss and inflammation.

The concept that the complement pathway is reactivated in pathological condition has been elegantly demonstrated in animal model of AD and in AD patients, correlated with a reduced spine density [18]. In human epileptic tissue, Wyatt et al. [23] documented microglia-dendritic contact associated with C1q expression more pronounced in areas with hypertrophic/amoeboid microglia in comparison with tissue not affected by epilepsy used as controls. Nevertheless, information concerning spines/synapse density were not available in this study and the etiology was not clear. By combining spine density and microglia-dendrite interaction, we provide additional support to the possibility of a reactivation of pruning activity as a cause of spine loss; this mechanism seems not to be always present in epilepsy and is pathology/tissue dependent. To reinforce this hypothesis, we used organotypic cultures from human surgical specimens that did not show FCD features. We studied the effect of complement protein administration on dendritic spines visualized by using DiI fluorescent probe; this method is useful to label plasma membrane of cells and provides high-quality staining of individual neurons and excellent dendritic spines resolution [38]. First, we demonstrated similar spine density in not cultured slices (baseline) and in nontreated cultured slices, suggesting that the tissue manipulation did not affect this measurement. Notably, the spine density in these controls was similar to that observed in our previous work in nondysplastic cases using Golgi method [10]. When cultured slices were treated with complement proteins, qualitative and quantitative data showed a trend of reduction in spine density along dendritic segments but no statistical analysis was possible due to the limited number of data. The main problems were (i) the surgical tissue availability, different in the different cases, which was responsible for the different number of slices analyzed, and (ii) several technical pitfalls we encountered in some time points. However, we want to point out that human brain tissues obtained after surgery are rarely used for functional studies, which usually use acutely prepared

slices [39]. In particular, the organotypic culture technique applied to adult tissues is more challenging and it has been rarely utilized in experimental works mainly because surgical material is not commonly available [40,41].

All these evidences suggest that components of the complement cascade and microglia can mediate the dendritic spine loss observed in Type II FCD. However, we want to notice that in other genetic neurological disorders also presenting dendritic and spine pathology, different mechanisms may be involved [42,43]. What initiates complement activation in Type II FCD is an important and unanswered question. Multiple evidences report brain mosaicism with mTOR-related pathogenic variants in resected dysplastic tissues [44]. The activation of mTOR pathway is critical for the development of immune cells in the CNS, as well as many processes of immune cells are regulated by mTOR signaling [45]. Changes in mTOR signaling and immune system may initiate the complement activation in TYPE IIb FCD, suggesting that complement proteins could be interesting targets for novel therapeutics approach in these forms of epilepsy.

#### AUTHOR CONTRIBUTIONS

Laura Rossini and Rita Garbelli contributed to the original research idea and conception, study design, literature search, data collection and article drafting. Dalia De Santis, and Erica Cecchini contributed to the neuropathological evaluation of the surgical specimens. Cinzia Cagnoli, Emanuela Maderna, and Daniele Cartelli contributed to conducting experiments and data acquisition. Bryan Paul Morgan and Megan Torvell contributed to data interpretation and to the final version of the article. Roberto Spreafico, Roberta Di Giacomo, Marco de Curtis, and Laura Tassi provided clinical data, supervised the study and contributed to critical revision of the article. All authors provided intellectual content and a critical review of the article.

#### ACKNOWLEDGMENTS

The study was supported by AICE-FIRE grant (to Laura Rossini) and the Italian Ministry of Health grant RF-2016-02362195 (to Roberta di Giacomo). We also acknowledge Dr F. Deleo for his help in statistical analysis.

#### CONFLICT OF INTEREST

The authors declare that they have no conflicts of interest.

#### DATA AVAILABILITY STATEMENT

All data provided in this study are available from the corresponding author upon a reasonable requirement.

#### ORCID

Laura Rossini  <https://orcid.org/0000-0003-3571-8779>

Dalia De Santis  <https://orcid.org/0000-0002-2519-2067>

Cinzia Cagnoli  <https://orcid.org/0000-0001-6863-6687>

Emanuela Maderna  <https://orcid.org/0000-0002-5736-3166>

Daniele Cartelli  <https://orcid.org/0000-0002-7069-420X>

Bryan Paul Morgan  <https://orcid.org/0000-0003-4075-7676>

Megan Torvell  <https://orcid.org/0000-0003-3789-1452>

Roberto Spreafico  <https://orcid.org/0000-0002-6528-1240>

Roberta di Giacomo  <https://orcid.org/0000-0003-4202-955X>

Laura Tassi  <https://orcid.org/0000-0002-0632-7296>

Marco de Curtis  <https://orcid.org/0000-0001-7443-6737>

Rita Garbelli  <https://orcid.org/0000-0002-6475-4974>

## REFERENCES

- Spruston N. Pyramidal neurons: dendritic structure and synaptic integration. *Nat Rev Neurosci*. 2008;9:206–21.
- Khanal P, Hotulainen P. Dendritic spine initiation in brain development, learning and diseases and impact of BAR-domain proteins. *Cell*. 2021;10:2392.
- Calabrese B, Wilson MS, Halpain S. Development and regulation of dendritic spine synapses. *Physiology (Bethesda)*. 2006;21:38–47.
- Cardozo PL, de Lima IBQ, Maciel EMA, Silva NC, Dobransky T, Ribeiro FM. Synaptic elimination in neurological disorders. *Curr Neuropharmacol*. 2019;17:1071–95.
- Blumcke I, Zusratter W, Schewe JC, et al. Cellular pathology of hilar neurons in Ammon's horn sclerosis. *J Comp Neurol*. 1999;414:437–53.
- Freiman TM, Eismann-Schweimler J, Froscher M. Granule cell dispersion in temporal lobe epilepsy is associated with changes in dendritic orientation and spine distribution. *Exp Neurol*. 2011;229:332–8.
- Multani P, Myers RH, Blume HW, Schomer DL, Sotrel A. Neocortical dendritic pathology in human partial epilepsy: a quantitative Golgi study. *Epilepsia*. 1994;35:728–36.
- Vaquero J, Qya S, Cabezudo JM, Bravo G. Morphological study of human epileptic dendrites. *Neurosurgery*. 1982;10:720–4.
- Belichenko PV, Dahlstrom A. Studies on the 3-dimensional architecture of dendritic spines and varicosities in human cortex by confocal laser scanning microscopy and Lucifer yellow microinjections. *J Neurosci Methods*. 1995;57:55–61.
- Rossini L, De Santis D, Mauceri RR, et al. Dendritic pathology, spine loss and synaptic reorganization in human cortex from epilepsy patients. *Brain*. 2021;144:251–65.
- Swann JW, Al-Noori S, Jiang M, Lee CL. Spine loss and other dendritic abnormalities in epilepsy. *Hippocampus*. 2000;10:617–25.
- Wong M. Modulation of dendritic spines in epilepsy: cellular mechanisms and functional implications. *Epilepsy Behav*. 2005;7:569–77.
- Stevens B, Allen NJ, Vazquez LE, Howell GR, Christopherson KS, Nouri N, et al. The classical complement Cascade mediates CNS synapse elimination. *Cell*. 2007;131:1164–78.
- Stephan AH, Madison DV, Mateos JM, Fraser DA, Lovelett EA, Coutellier L, et al. A dramatic increase of C1q protein in the CNS during Normal aging. *J Neurosci*. 2013;33(33):13460–74.
- Miyamoto A, Wake H, Moorhouse AJ, Nabekura J. Microglia and synapse interactions: fine tuning neural circuits and candidate molecules. *Front Cell Neurosci*. 2013;7:70.
- Propson NE, Gedam M, Zheng H. Complement in neurologic disease. *Annu Rev Pathol*. 2021;24(16):277–98.
- Schartz D, Tenner AJ. The good, the bad, and the opportunities of the complement system in neurodegenerative disease. *J Neuroinflammation*. 2020;17(1):354.
- Dejanovic B, Huntley MA, De Maziere A, et al. Changes in the synaptic proteome in Tauopathy and Rescue of tau-Induced Synapse Loss by C1q antibodies. *Neuron*. 2018;100(6):1322–1336.e7.
- Watkins LM, Neal JW, Loveless S, Michailidou I, Ramaglia V, Rees MI, et al. Complement is activated in progressive multiple sclerosis cortical grey matter lesions. *J Neuroinflammation*. 2016;13(1):161.
- Laskaris L, Zalesky A, Weickert CS, di Biase MA, Chana G, Baune BT, et al. Investigation of peripheral complement factors across stages of psychosis. *Schizophr Res*. 2019;204:30–7.
- Aronica E, Boer K, van Vliet EA, Redeker S, Baayen JC, Spliet WGM, et al. Complement activation in experimental and human temporal lobe epilepsy. *Neurobiol Dis*. 2007;26(3):497–511.
- Boer K, Jansenc F, Nellist M, et al. Inflammatory processes in cortical tubers and subependymal giant cell tumors of tuberous sclerosis complex. *Epilepsy Res*. 2008;78(1):7–21.
- Wyatt SK, Witt T, Barbaro NM, Cohen-Gadol AA, Brewster AL. Enhanced classical complement pathway activation and altered phagocytosis signaling molecules in human epilepsy. *Exp Neurol*. 2017;295:184–93.
- Gruber VE, Luinenburg MJ, Colleselli K, Endmayr V, Anink JJ, Zimmer TS, et al. Increased expression of complement components in tuberous sclerosis complex and focal cortical dysplasia type 2B brain lesions. *Epilepsia*. 2022;63(2):364–74.
- Engel JJ, Van Ness P, Rasmussen TB, Ojemann LM. Outcome with respect to epileptic seizures. New York, NY: Raven Press; 1993. p. 553–71.
- Loveless S, Neal JW, Howell OW, Harding KE, Sarkies P, Evans R, et al. Tissue microarray methodology identifies complement pathway activation and dysregulation in progressive multiple sclerosis. *Brain Pathol*. 2018;28(4):507–20.
- Eriksson SH, Free SL, Thom M, et al. Correlation of quantitative MRI and neuropathology in epilepsy surgical resection specimens—T2 correlates with neuronal tissue in gray matter. *NeuroImage*. 2007;37(1):48–55.
- Le Duigou C, Savarya E, Morin-Brureau M, et al. Imaging pathological activities of human brain tissue in organotypic culture. *J Neurosci Methods*. 2018;298:33–44.
- Rossini L, Garbelli R, Gnatkovsky V, Didato G, Villani F, Spreafico R, et al. Seizure activity per se does not induce tissue damage markers in human neocortical focal epilepsy. *Ann Neurol*. 2017;82:331–41.
- Muhlebauer A, Coras R, Kobow K, et al. Neuropathologic measurements in focal cortical dysplasias: validation of the ILAE 2011 classification system and diagnostic implications for MRI. *Acta Neuropathol*. 2012;123(2):259–72.
- Orlova KA, Crino PB. The tuberous sclerosis complex. *Ann N Y Acad Sci*. 2010;1184:87–105.
- Crino PB. Evolving neurobiology of tuberous sclerosis complex. *Acta Neuropathol*. 2013;125(3):317–32.
- Iyer A, Zurolo E, Spliet WGM, van Rijen PC, Baayen JC, Gorter JA, et al. Evaluation of the innate and adaptive immunity in type I and type II focal cortical dysplasias. *Epilepsia*. 2010;51(9):1763–73.
- Zimmer TS, Broekaart DWM, Luinenburg M, Mijnsbergen C, Anink JJ, Sim NS, et al. Balloon cells promote immune system activation in focal cortical dysplasia type 2b. *Neuropathol Appl Neurobiol*. 2021;47(6):826–39.
- Tassi L, Garbelli R, Colombo N, Bramerio M, Russo GL, Mai R, et al. Electroclinical, MRI and surgical outcomes in 100 epileptic patients. *Epileptic Disord*. 2012;14(3):257–66.
- Presumey J, Bialas AR, Carroll MC. Complement system in neural synapse elimination in development and disease. *Adv Immunol*. 2017;135:53–79.
- Patel DC, Tewari BP, Chaunsali L, Sontheimer H. Neuron-glia interactions in the pathophysiology of epilepsy. *Nat Rev Neurosci*. 2019;20(5):282–97.
- Bączynska E, Pels KK, Basu S, Włodarczyk J, Ruszczycki B. Quantification of dendritic spines remodeling under physiological stimuli and in pathological conditions. *Int J Mol Sci*. 2021;22(8):4053.



39. Avoli M, Williamson A. Functional and pharmacological properties of human neocortical neurons maintained in vitro. *Prog Neurobiol.* 1996;48(6):519–54.
40. Eugène E, Cluzeaud F, Cifuentes-Diaz C, Fricker D, le Duigou C, Clemenceau S, et al. An organotypic brain slice preparation from adult patients with temporal lobe epilepsy. *J Neurosci Methods.* 2014;235:234–44.
41. Gonzales-Martinez JA, Bingaman WE, Toms SA, Najm IM. Neurogenesis in the postnatal human epileptic brain. *J Neurosurg.* 2007;107(3):628–35.
42. Carpenter JC, Männikkö R, Heffner C, Heneine J, Sampedro-Castañeda M, Lignani G, et al. Progressive myoclonus epilepsy KCNC1 variant causes a developmental dendritopathy. *Epilepsia.* 2021;62(5):1256–67.
43. Takashima S, Becker LE, Armstrong DL, Chan F. Abnormal neuronal development in the visual cortex of the human fetus and infant with down's syndrome. A quantitative and qualitative Golgi study. *Brain Res.* 1981;225(1):1–21.
44. Jesus-Ribeiro J, Pires LM, Melo JD, Ribeiro IP, Rebelo O, Sales F, et al. Genomic and epigenetic advances in focal cortical dysplasia types I and II: a scoping review. *Front Neurosci.* 2021; 14:580357.
45. Hodges SL, Lugo JN. Therapeutic role of targeting mTOR signaling and neuroinflammation in epilepsy. *Epilepsy Res.* 2020;161:106282.

## SUPPORTING INFORMATION

Additional supporting information can be found online in the Supporting Information section at the end of this article.

**How to cite this article:** Rossini L, De Santis D, Cecchini E, Cagnoli C, Maderna E, Cartelli D, et al. Dendritic spine loss in epileptogenic Type II focal cortical dysplasia: Role of enhanced classical complement pathway activation. *Brain Pathology.* 2022. e13141. <https://doi.org/10.1111/bpa.13141>